

EVOLUTION AND LIFETIME OF TRANSIENT CLUMPS IN THE TURBULENT INTERSTELLAR MEDIUM

D. FALCETA-GONÇALVES^{1,2} AND A. LAZARIAN²

¹ Escola de Artes, Ciências e Humanidades, Universidade de São Paulo-Rua Arlindo Bettio 1000, CEP 03828-000, São Paulo, Brazil

² Astronomy Department, University of Wisconsin, Madison, 475 North Charter Street, WI 53711, USA

Received 2011 January 25; accepted 2011 April 11; published 2011 June 22

ABSTRACT

We study the evolution of dense clumps and provide an argument that the existence of the clumps is not limited by their crossing times. We claim that the lifetimes of the clumps are determined by turbulent motions on a larger scale, and we predict the correlation of clump lifetime with column density. We use numerical simulations to successfully test this relation. In addition, we study the morphological asymmetry and the magnetization of the clumps as functions of their masses.

Key words: ISM: clouds – ISM: kinematics and dynamics – magnetohydrodynamics (MHD) – methods: numerical – stars: formation

Online-only material: color figure

1. INTRODUCTION

Star formation (SF) is believed to take place in collapsing cores within molecular clouds. These dense structures, however, are turbulent and magnetized. Both of these physical properties, allied to the gas thermal pressure, help support the cores against gravitational collapse. In the past few years, many authors have worked on this interesting subject, but many issues remain. One such issue concerns the true lifetimes of dense clumps in the interstellar medium (ISM). Evaporation, instabilities, and the turbulence itself are believed to destroy and fragment the clumps at short timescales comparable to the sonic/Alfvénic crossing timescales. On the other hand, gravitationally unstable cores should also fragment and collapse at even shorter timescales $< 10^5$ yr. These short timescales contradict observations of star-forming regions and also render the formation of massive stars virtually impossible.

The ISM is known to be turbulent (Armstrong et al. 1995; Elmegreen & Scalo 2004; Chepurnov & Lazarian 2010) with interstellar gas exhibiting a wide variety of structures, including giant molecular clouds (GMCs) at large scales and cloudlets or clumps at small scales. SF is believed to be triggered within these dense clumps; therefore, the understanding of the formation of these structures and their dynamic evolution is crucial to theories of SF and its efficiency in the ISM.

In the fragmentation model (Elmegreen & Mathieu 1983), it is assumed that the molecular clouds collapse due to their gravity, as the thermal energy is continuously reduced by the emission of radiation. During this process the gas temperature decreases while the density increases, and the Jeans mass $m_J(M_\odot) \simeq 10n^{-1/2}T^{3/2}$, with temperature T in Kelvin and gas density n in cm^{-3} , is reduced, resulting in cloud fragmentation. This process should occur up to scales where the opacity becomes too large and the radiative cooling inefficient. In such a scenario the dynamics of the plasma plays a minimal role. However, it is well known that molecular clouds are formed in supersonic turbulence, and the typical physical energies may be estimated as follows:

$$E_{\text{grav}} \simeq \frac{3Gm_c^2}{5R} \sim 10^{47} \text{ erg},$$

$$E_{\text{thermal}} \simeq \frac{2\pi nkTR^3}{3} \sim 10^{47} \text{ erg},$$

$$E_{\text{turb}} \simeq \frac{1}{2}m_c c_s^2 M_s^2 \sim 3 \times 10^{46} M_s^2 \text{ erg} \quad (1)$$

for a typical GMC of $m_c = 10^4 M_\odot$, $T = 20$ K, $R = 25$ pc, where c_s is the isothermal speed of sound and $M_s = u_{\text{turb}}/c_s$ is the averaged sonic Mach number of the turbulent eddies. For molecular clouds, observations provide typical values of $M_s \simeq 3\text{--}20$ (Larson 1981; Li & Houde 2008), resulting in supersonic turbulence at most of the molecular clouds. Though gravity continues to be the main cause of clump contraction and SF, the distribution of cloud sizes and masses may depend primarily on the turbulence itself. From the theoretical point of view, magnetohydrodynamic (MHD) simulation has been extensively used for studying the statistics of density distribution in turbulent plasmas (e.g., Ballesteros-Paredes et al. 1999; Padoan et al. 2003; Kowal et al. 2007; Burkhart et al. 2009), all presenting density and column density probability density functions similar to those observed, i.e., with density contrasts between the large-scale cloud and the dense cores of $\rho_{\text{core}}/\langle\rho\rangle \sim 10^2\text{--}10^4$, in the supersonic turbulent flows.

These dense structures that are not gravitationally dominated are believed to be transient and, most importantly, short lived (Kirk et al. 2005). A fraction of these clumps are believed to present masses larger than the Jeans mass and are subject to fast collapse, with a collapsing free-fall time estimated as $t_{\text{ff}} = 3.4 \times 10^7 n^{-0.5} \sim 10^4\text{--}10^5$ yr. This value is too short compared to the lifetimes required for the formation of high-mass stars ($t > 10^5$ yr; Churchwell 2002; Mac Low & Klessen 2004). For this reason, several supporting mechanisms other than thermal pressure have been proposed. Observationally, the turbulent flows in molecular clouds are supersonic at scales $l > 0.05$ pc and have been invoked as the main support mechanisms against the gravitational collapse of the clouds (Bonazzola et al. 1987; Xie et al. 1996). Magnetic fields also play a major role in this process, in that the uniform component of a field supports the cloud in the perpendicular direction (Mestel & Spitzer 1956; McKee & Zweibel 1995; Gammie & Ostriker 1996; Martin et al. 1997), the perturbations (primarily the Alfvénic mode) being responsible for the extra pressure in the parallel direction (see Falceta-Gonçalves et al. 2003). In both

cases, since turbulence also excites the Alfvénic modes within molecular clouds, turbulence must exist for $t > 10^5$ yr. One important issue is that turbulence decays in a relatively short timescale $t_{\text{damp}} \sim l/v \sim 10^3\text{--}10^4$ yr, where $l \sim 0.1$ pc is the turbulent cell size and $v \sim 5 \text{ km s}^{-1}$ is its turnover speed. Clouds that are not collapsing are believed to be quickly destroyed as well, either by instabilities such as Kelvin–Helmholtz (Kamaya 1996), shocks, or evaporation. This fact motivates a study of the dynamics of clump evolution investigating the origin of these dense regions and how long the clumps survive in a turbulent medium.

In this work, we study, based on numerical simulations, the formation and the dynamic evolution of the transient dense regions in molecular clouds. We concentrate on the survival of clumps through shocks and turbulent diffusion. We also discuss, based on the simulations, the origin and morphology of the identified dense structures. In Section 2, we describe the code and basic assumptions used to obtain the results, which are shown in Section 3. In Section 4, we discuss the main results and present the conclusions of this work, followed by the summary in Section 5.

2. CODE DESCRIPTION

The gas in starless molecular clouds may be considered isothermal, but self-gravity may play a major role in its dynamics. In this work, however, we disregard gravitational force and consider exclusively the effects of turbulence in the formation and destruction of dense clumps.

The simulations are performed solving the set of ideal MHD isothermal equations, in conservative form, as follows:

$$\frac{\partial \rho}{\partial t} + \nabla \cdot (\rho \mathbf{v}) = 0, \quad (2)$$

$$\frac{\partial \rho \mathbf{v}}{\partial t} + \nabla \cdot \left[\rho \mathbf{v} \mathbf{v} + \left(p + \frac{B^2}{8\pi} \right) \mathbf{I} - \frac{1}{4\pi} \mathbf{B} \mathbf{B} \right] = \mathbf{f}, \quad (3)$$

$$\frac{\partial \mathbf{B}}{\partial t} - \nabla \times (\mathbf{v} \times \mathbf{B}) = 0, \quad (4)$$

$$\nabla \cdot \mathbf{B} = 0, \quad (5)$$

$$p = c_s^2 \rho; \quad (6)$$

where ρ , \mathbf{v} , and p are the plasma density, velocity, and pressure, respectively; $\mathbf{B} = \nabla \times \mathbf{A}$ is the magnetic field; \mathbf{A} is the vector potential; and $\mathbf{f} = \mathbf{f}_{\text{turb}}$ represents the external source terms, such as the turbulence forcing. The code solves the set of MHD equations using a Godunov-type scheme, based on a second-order-accurate and essentially non-oscillatory spatial reconstruction. We use the Harten–Lax–van Leer Riemann solver for shock capturing, and the magnetic divergence is assured by the constrained transport method for the induction equation. The code has been extensively tested (Falceta-Gonçalves et al. 2008; Leão et al. 2009; Burkhart et al. 2009; Kowal et al. 2009; Falceta-Gonçalves et al. 2010a, 2010b). The turbulence is triggered by the injection of solenoidal perturbations in Fourier space of the velocity field.

We run six models with a numerical resolution of 512^3 cells, in a fixed uniform grid, at different turbulent regimes, ranging from subsonic to supersonic and sub- to super-Alfvénic, which were already presented in Falceta-Gonçalves et al. (2010c). The

box size corresponds to $L_{\text{box}} = 10$ pc, the assumed average number density of the gas $n_{\text{H}} = 10^2 \text{ cm}^{-3}$, the magnetic field strength $B \sim 2 \mu\text{G}$, and $T \sim 20$ K.

3. RESULTS

The numerical simulations show a dynamic picture with clumps changing their locations and shapes. As discussed in Kowal et al. (2007), the density contrast $\rho/\bar{\rho}$ proportionally follows the sonic Mach number, with little dependence on the Alfvénic Mach number. As the focus of this work is on the dynamics of the dense structures, we focus our calculations on the supersonic case (Model 3 of Falceta-Gonçalves et al. 2010c). This specific run presents an average sonic Mach number $M_s = 7.2$ and shows $\rho/\bar{\rho} \sim 1000\text{--}5000$ depending on the snapshot. The initial magnetic field is uniformly set with $\beta = P_{\text{thermal}}/P_{\text{mag}} = 1$. The dynamic evolution of clumps is studied based on 100 snapshots per dynamic time $t_D = L/v_L$, and the simulation is performed up to $t = 5t_D$.

3.1. Identification and Origin of Clumps

We identify the clumps in a very simple way, using isocontours of density. The clump identification method determines, for each snapshot, all cells of the simulated cube with density above a given threshold $\rho'_{\text{min}} = \rho/\bar{\rho}$. All other cells with $\rho < \rho'_{\text{min}}$ are flagged and not used. The program then identifies as a single clump the region with all neighboring overdense cells. This procedure is similar to the one described in Schmidt et al. (2010), with a difference being that the limit of the clump size is given by its total mass rather than the boundary density. In Figure 1, we show the clumps identified at $t = 4t_D$ for two different thresholds: $\rho'_{\text{min}} = 20$ and 30.

At each snapshot, different clumps, varying both in size and location, are identified. In order to follow the dynamics of each clump we must determine the displacement of a clump from $t_1 = t'$ to the subsequent frame $t_2 = t' + \Delta t$. Our method uses the local averaged velocity field to estimate future positions of the clump. At $t = t'$, for each clump, the average velocity $\mathbf{u} = \Sigma_N \mathbf{v}_i / N$ is obtained. The estimated location of each cell of the given clump is then obtained by $\mathbf{x}_i = \mathbf{x}_i^0 + \mathbf{u} \Delta t$. At snapshot t_2 , the same procedure is executed. At t_2 if a clump—or part of it—is identified within the region defined by \mathbf{x}_i , it is flagged as an old clump that is simply evolving. If more than one clump is identified in the region defined by \mathbf{x}_i , then two different possibilities are considered: (1) the clump has fragmented, or (2) a different clump has moved to occupy this region. If the second condensation is not also located at the other set of \mathbf{x}_i , determined from a different clump at $t = t'$, it may be considered a fragment.

From the velocity field, it is also possible to determine the origin of the condensations. Transient clumps may be produced by accumulating matter in a supersonic flow. The converging flows of the gas may have different origins, including locally “colliding flows”³ (Elmegreen 1993; Blitz & Williams 1997) or isothermal shocks (Beresnyak et al. 2005). In Figure 2, we show two maps. One is for the divergence of velocity, and the other shows density peaks. The correlation between the two clarifies the origin of the gas clumpiness. The strong divergence of velocity at the peaked density (mostly at the edges) indicates that shocks are responsible for their formation. Visually, one

³ The proper idea is that thinking of converging flows as “colliding flows” may induce the reader to the erroneous impression that separate jet-like flows are common in developed turbulence.

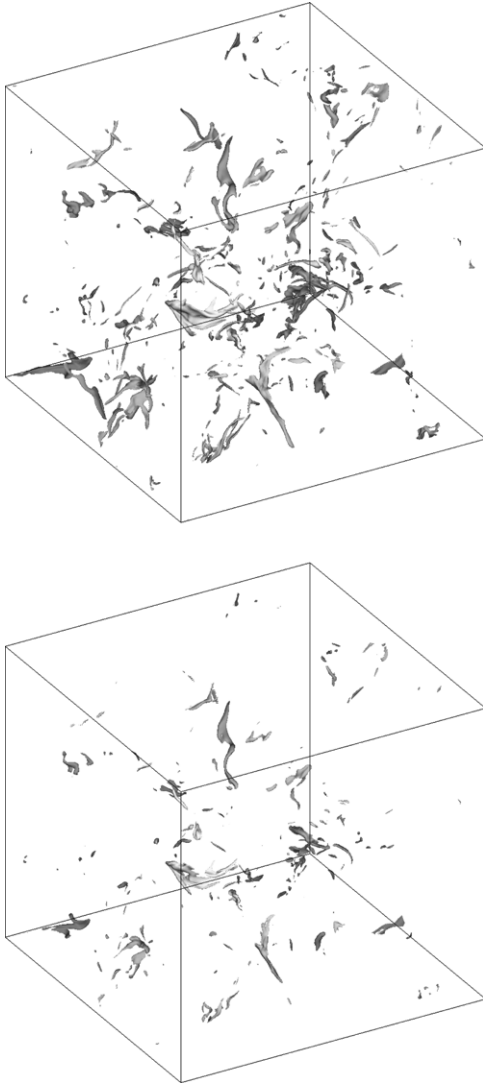


Figure 1. Visualization of the overdense regions of the simulation at snapshot $t = 4t_D$ for thresholds $\rho'_{\min} = 20$ and 30.

can verify that the majority of the clumps are associated with shocks. At the center of the image, a vertical shock is formed but is uncorrelated to a density peak. The reason for this is its evolutionary stage. In subsequent frames the density increases and the shock region is recognized.

3.2. Morphology and Magnetic Fields

Additionally, the clump finding routine was developed to measure clump dimensions and morphology. Two dimensions are determined including the lengths along and perpendicular to the mean magnetic field within the condensation. The asymmetry of the cloud is calculated as the ratio between the two lengths $A = L_{\parallel}/L_{\perp}$. The average ratio of the gas and magnetic pressures within the cloud, β , is also obtained for each structure. The results for all clumps found by this method are shown in Figure 3. In the figure, M is the mass of the clump, normalized by solar masses.

We observe that most clumps are found to be compressed along the mean magnetic field, i.e., they are larger in the perpendicular direction. However, there is a selection effect with the cloud mass. Clumps with small mass ($M_{\text{clump}} < 3 M_{\odot}$) tend to be larger in the parallel direction, and the most massive

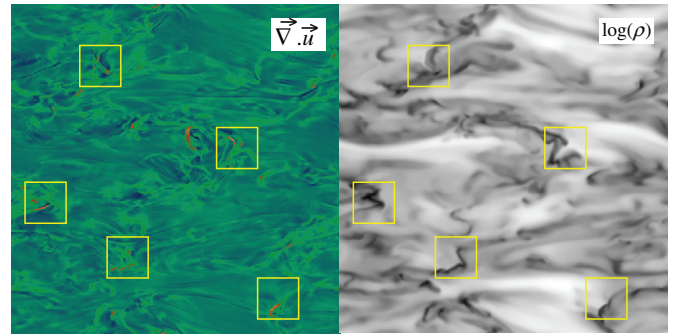


Figure 2. For a central slice at $t = 4t_D$, the left panel shows the divergence of the velocity field, and the right panel shows the logarithm of the gas density. Boxes are used to show the regions where we observe obvious correspondence of structures.

(A color version of this figure is available in the online journal.)

cores tend to be isotropic ($M_{\text{clump}} > 200 M_{\odot}$). Following the theory for compressible MHD turbulence, the Alfvénic part of perturbations scales as $l_{\parallel} \sim l_{\perp}^{2/3}$ (see Goldreich & Sridhar 1995 and numerical tests of Cho & Lazarian 2002, 2003; Kowal & Lazarian 2010). At the smaller scales, the low (subsonic) velocity, since $v_l \sim l^{1/3}$, results in a coupling between the density and velocity fields. Since the velocity fields are anisotropic and aligned with the local field, the density acts as an almost passive scalar aligning to the magnetic field lines as well. At intermediate/larger scales the supersonic motions result in the gas compression. The shock surfaces are mostly perpendicular to the magnetic field for two reasons: (1) the shocks parallel to the field are weakened by the magnetic pressure, resulting in smaller contrast of density; and (2) the velocity anisotropy results in larger velocity components at the parallel direction, producing stronger shocks with density surfaces perpendicular to the field lines. At the other end, i.e., the most massive cores, the turbulence is strongly super-Alfvénic and the field mostly random. In this case, neither the velocity nor the density present anisotropic distribution.

Figure 3 also presents the averaged β value for all clumps followed in this simulation. There is a clear anticorrelation between the total mass of the clump and β . An interesting effect is that the asymmetry of clumps and their β for the range of masses follow a very similar fashion, i.e., they decrease with the increase of the mass of a clump, except for larger masses. We may interpret this as an effect of shearing of clumps by Alfvénic motions. We start the run with equal thermal and magnetic pressures, i.e., $\beta = 1$. The magnetic pressure tends to increase within the clumps, making them magnetically dominated. Turbulent motions, in general, result in compression of the magnetic field with $B \propto n^{\alpha}$, with $\alpha \sim 0.5-1.0$ (Burkhart et al. 2009). Since $P_{\text{th}} \propto n$ and $P_{\text{mag}} \propto B^2$, as the gas becomes more compressed, β becomes lower.

3.3. Clump Lifetimes

How long do the clumps live? The answer to this question is important for many astrophysical issues, such as core collapse, SF, and SF efficiency. As mentioned above, it has in the past few years become common to invoke the shortest of the sonic and Alfvénic crossing times as an estimation of the cloud survival timescale, which is then compared to the free-fall or ambipolar diffusion timescales.

From the simulation it is possible to track the evolution of individual clumps, determining the times of formation and

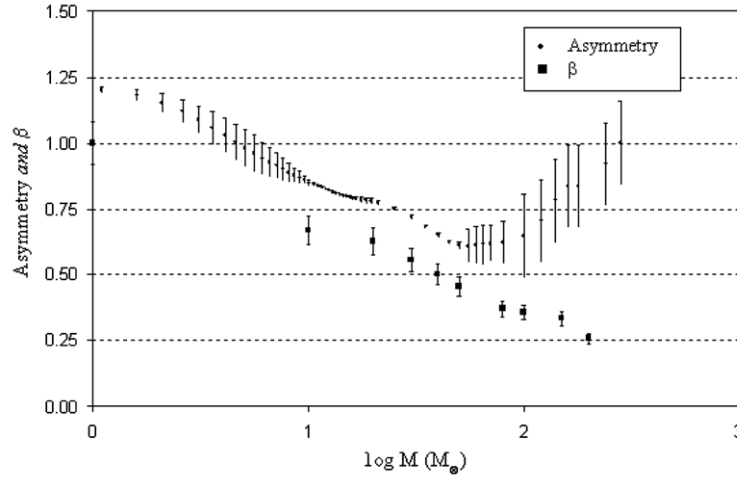


Figure 3. Asymmetry of dimensions parallel and perpendicular to the mean magnetic field ($A = L_{\parallel}/L_{\perp}$), and averaged $\beta = P_{\text{th}}/P_{\text{mag}}$, for the clumps with respect to the total mass of the clump in solar masses.

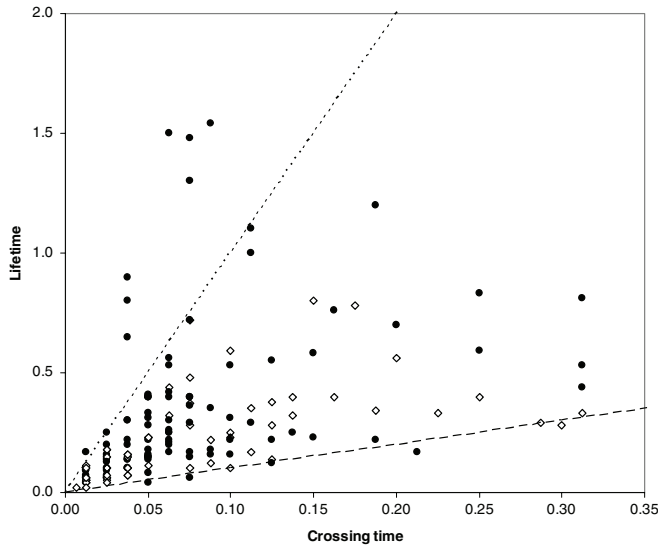


Figure 4. Survival times determined for all the cores identified for both thresholds $\rho'_{\text{min}} = 20$ (open circles) and 30 (filled circles). The lifetimes are given in terms of the sonic crossing time $\tau_s = l_{\text{clump}}/c_s$, which is shown in the abscissae. The dashed line corresponds to $t_{\text{life}} = \tau_s$, and the dotted line corresponds to $t_{\text{life}} = 10\tau_s$.

destruction. In Figure 4, we show the cores identified for both thresholds $\rho'_{\text{min}} = 20$ (open circles) and 30 (filled circles). The dashed line corresponds to $t_{\text{life}} = \tau_s$, where $\tau_s = l_{\text{clump}}/c_s$, and the dotted one corresponds to $t_{\text{life}} = 10\tau_s$. There is a correlation between the two timescales, showing that larger cores are long-lived compared to the smaller ones. The same conclusion is valid for the denser cores, as we compare two cores with similar sizes (similar τ_s) but different density thresholds. The filled circles ($\rho'_{\text{min}} = 30$) populate an upper region in this plot compared to the open circles ($\rho'_{\text{min}} = 20$).

As seen in Figure 3, the clumps tend to be magnetically dominated. Therefore, we expect the shortest timescale to be $t_A = l/V_A$, where l is the clump size and V_A is the Alfvén velocity. However, we see in Figure 4 that most of the clumps live longer than the sonic crossing time τ_s . In fact, most of the clumps live between 1 and $10\tau_s$, which, if we combine the results on plasma β of the clumps, translates into the range from 1 to $20t_A$.

This result is especially important for the formation of dense and massive cores. As mentioned above, for the ISM the collapse timescales of dense cores (even considering the ambipolar diffusion) tend to be fast enough to prevent the accumulation of material, e.g., massive stars to form. It is important that it survives longer than $\sim t_{\text{cross}}$. A rough estimate of the gas accumulating in a high Mach number flow can be obtained by assuming that the compressible turbulent motions of size l and density ρ_l accumulate gas as

$$\rho v_L \tau_l \sim \rho_l l, \quad (7)$$

where v_L is the velocity of the flow at the energy injection scale and ρ is the density of the unperturbed gas. This provides an estimate for the time to accumulate the material of the clump:

$$\tau_l \sim \frac{\rho_l l}{\rho v_L}, \quad (8)$$

which indicates that the characteristic lifetime of the clump is actually determined by the longer timescales associated with the compressible flows.

Examining Equation (8) we see that, contrary to widespread belief, that clumps may survive much longer than the sound crossing time. We see that clumps may accumulate matter for as long as the large-scale converging flow exists. The latter may proceed up to the injection time L/v_L . In the proposed model, the accumulated column density of a clump is proportional to $\rho_l l$ and is also proportional to the time the compressible converging flow accumulates the material.

To test this simple idea we calculate the column density of each of the clumps and relate it to their lifetimes. In order to obtain an estimation of the column density—which does not depend on any specific orientation of a given line of sight—we calculate the averaged dimension of each cloud and multiply by its averaged density, i.e., $\Sigma \sim \bar{n}_c \bar{l}_c$. The result is shown in Figure 5 in real physical units. The solid line shows a good linear relationship between the two quantities, $\tau_{\text{life}} \propto \Sigma$. The dispersion is expected due to the crude nature of our definition of a clump. A formal fit to the data using linear regression gives $\alpha = 0.72 \pm 0.08$. The power index obtained from the statistical fit is similar to our prediction. If only the clumps with threshold $\rho'_{\text{min}} = 20$ are considered, the linear regression gives

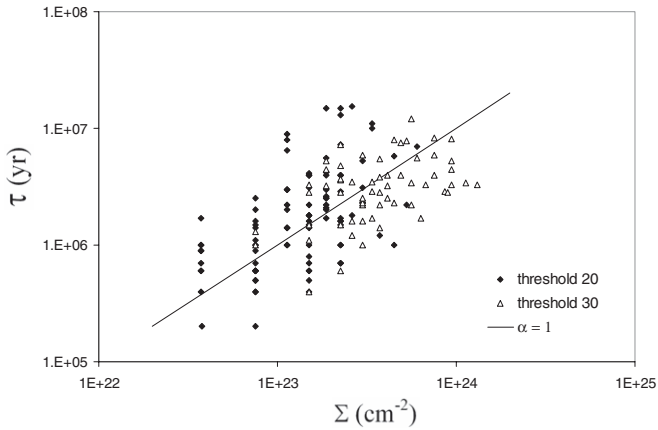


Figure 5. Relationship between the lifetime of a clump and its column density. The solid line is given as a reference and corresponds to a linear relationship $\tau_{\text{life}} \propto \Sigma^a$, with $a = 1$.

$\alpha = 0.81 \pm 0.12$, which is even closer to our prediction. The discrepancy between the predicted scaling and the statistical fit may be due to a completeness effect. It is possible that there is a lack of clumps in the top right region of the plot, i.e., denser clumps that survive longer, simply because of limited numerical resolution that artificially introduces a large viscosity in the system. As a consequence, the small clumps are more easily destroyed. Further simulations with finer resolution, or better schemes, are recommended in order to test this possibility.

3.4. Clump Evaporation Versus Turbulent Disruption

The dense clumps formed within molecular clouds may be subject to gas evaporation. This process happens once there is no pressure equilibrium between the denser core and the surrounding material of the cloud. In the case of starless cores, we may consider that the molecular cloud plasma is shielded from background radiation and the gas is approximately isothermal. The contrast of density is then responsible for a pressure gradient resulting in evaporation. In such a case, thermal conduction is not the dominant physical process for the gas evaporation but the gas diffusion, i.e., the flow from the cores, to the less dense regions.

A crude estimate of the clump evaporation rate may be obtained (see Cowie & McKee 1977). We assume a spherical clump, in a quasi-stationary approximation, that follows the momentum equation given as

$$\rho v \frac{\partial v}{\partial r} \simeq -\frac{\partial P}{\partial r}, \quad (9)$$

where ρ is the gas mass density, P is the pressure, and r is the distance to the center of the clump. Assuming the gas at the core and its surroundings is isothermal, as explained above, this equation is simplified as follows:

$$\frac{\partial \ln(\rho)}{\partial r} = -\frac{1}{2} \frac{\partial M^2}{\partial r}, \quad (10)$$

where M is the sonic Mach number of the gas flow, giving the solution

$$M^2 = 2 \ln \left(\frac{\rho_0}{\rho} \right). \quad (11)$$

The evaporation timescale is given by

$$\tau_{\text{evap}} \simeq \frac{m_c}{\dot{m}_{\text{evap}}}, \quad (12)$$

where m_c is the total mass of the clump and \dot{m}_{evap} is the mass-loss rate,

$$\dot{m}_{\text{evap}} = 4\pi r^2 \rho v. \quad (13)$$

Assuming a Gaussian radial distribution for the gas density within the clump, the evaporation timescale is reduced to

$$\tau_{\text{evap}} \simeq \frac{\sqrt{2}}{3} \frac{r_c^4}{r^3 c_s} \frac{1}{c_s} \exp \left(\frac{r^2}{2r_c^2} \right) \sim 3 \times 10^6 \text{ yr} \quad (14)$$

for a typical clump size obtained in the simulation of $r_c = 0.3$ pc, with $c_s = 1 \text{ km s}^{-1}$, and $r/r_c = 1/e$. This evaporation timescale of the clump is much larger compared to other dynamic scales of the systems, such as the sound and turbulent crossing times ($\sim 10\tau_{\text{sound}}$ and $\sim 30\tau_{\text{turb}}$). Therefore, we may conclude that gas evaporation is not the dominant destructive physical process for our clumps. In our simulations, though turbulence is the main process for the formation of the clumps, turbulent diffusion is also the main disruptive mechanism.

Turbulent disruption of clumps may be caused by ablation, fragmentation by strong shocks, and surface instabilities such as the Kelvin–Helmholtz instability that rises at the surface of the dense core as less dense plasma flows around it (see Pittard et al. 2010 and references therein). This effect is greatly increased in supersonic cases. All these processes occur simultaneously in the present simulation.

4. DISCUSSION

In this work, we present MHD numerical simulations of an isothermal turbulent ISM gas. We simulate the clumps formed by the turbulent supersonic gas and study their dynamic evolution and the dependence of their physical properties on the magnetization of the gas. As a result we observe a large dispersion of clump lifetimes and their sizes/masses. However, most importantly, we show that the dense cores survive for timescales larger than the sonic or Alfvénic crossing times ($t_{\text{life}} \sim 1\text{--}10\tau_s$ or $\sim 1\text{--}20\tau_A$). The origin of the dense cores in the simulation is attributed to shocks. A linear relation between the lifetime of the clumps and their column density was found. It may be interpreted as a direct consequence of the gas accumulation in a supersonic converging flow.

The most important single result of this study is the linear relation of the clump lifetime and the column density of the clump. This relation shows that the lifetime of a clump may be substantially longer than the sonic or Alfvén crossing time of the cloud. One may therefore speculate that the actual clumps of interstellar gas and even molecular clouds exist for timescales much longer than the crossing time. We remind the reader that the controversy about the lifetime of molecular clouds usually concerns the notion that the magnetic support of the clouds is predicted to provide the cloud lifetime of the order of $10t_A$. It is usually assumed that the transient turbulent formation of clumps implies the lifetime of the order is at minimum $1t_s$ or $1t_A$. Our simulations show that this is not true and that the correlation times of the large-scale flows play an important role in preserving the clouds. This conclusion is based on isothermal simulations; therefore, one may be concerned about its relevance in a different scenario. If the flows are not isothermal, as in our computation, the density of the clumps created would be different since the contrast of density decreases as the cooling becomes less efficient. However, the main result in terms of the correlation time of the flows should remain, because the converging flows that create clumps would still

be correlated to the turnover time of the large-scale eddies. Another initial parameter that may possibly cause different results is the Mach number of the injected turbulence. In a case with a low Mach number, the origin of the dense regions may be different, mostly due to the density perturbations by the slow and fast waves instead of accumulated material within a shock layer (Cho & Lazarian 2003). In this case, Equation (8) is expected to be no longer valid. A similar difference may arise when comparing strongly magnetized to weakly magnetized supersonic turbulence. This will be addressed in a future work.

This result may be compared to previous works. Vázquez-Semadeni et al. (2005) studied the evolution of cloud cores in subcritical, strongly magnetized, and supersonic turbulent flows. In their simulations most of the dense cores were seen to be extremely transient in nature, with lifetimes ranging from 0.01 to $0.075t_s$, with the exception of a few clumps that became gravitationally bound and survived for few local free-fall times. A possible explanation for the observed discrepancies in lifetimes is the lower numerical resolution. Vázquez-Semadeni et al. (2005) used 256^3 and 128^3 cubes in their analysis. Also, the shock-capturing method and the reconstruction method of the variables may play an important role in the diffusion of condensations. In this sense, more numerical tests with finer numerical resolutions and better solvers are mandatory.

Galván-Madrid et al. (2007) extended this work and studied the lifetimes of cores in prestellar phases. The prestellar lifetime of a core (t_{pre}) is defined as the interval between the time when it is first detected at a given threshold and the time when its peak density reaches the saturated value indicating further collapse and SF. In this case, these authors obtained t_{pre} in the range of $\sim 3\text{--}10\tau_{\text{ff}}$, which is similar to what was obtained in the present work.

Interestingly enough, the clumps we observe are very dynamic. Therefore, again extrapolating to molecular clouds, we may speculate that the issue of “support of turbulence” in molecular clouds may be artificially overemphasized. As long as the turbulent gas is being pushed into molecular cloud, it remains turbulent. An exception may be presented in the case of small clumps, over whose scale the effects of viscosity are important. Such clumps can accept a flow of matter from a large scale, in which the viscosity is important, but they are small enough to allow development of instabilities within the clump.

It is interesting that the lifetime of clumps scales with the column density. Larson’s scalings predict that clouds of different sizes tend to present a constant column density, though a few authors propose this to be an observational artifact (see Vázquez-Semadeni et al. 1997). We could interpret this result as the existence of the preferable lifetime of the clumps in a flow. Naturally, in the turbulent fluid such a scale is that of turbulence injection at large scale, namely, L/v_L .

The role of magnetic field in SF is a subject of much discussion. The approaches vary from statements on the absolute dominance of magnetic fields (see Shu et al. 1987) to its marginal importance in the presence of turbulence (see Padoan & Nordlund 1999). Our results show that one may expect an increase of magnetic to gaseous pressure as turbulence creates clumps. Obviously, this result depends on the physical assumptions made in these simulations. If the gas were not isothermal, and if the cooling process were inefficient, β should not increase with the clump density as much as we observed here. We believe that “reconnection diffusion” based on the ability of magnetic fields to reconnect in turbulent media (Lazarian & Vishniac 1999; Lazarian et al. 2004), enabling the diffusion of magnetic

field in relation to conducting fluid, is the process that can dominate ambipolar diffusion in many astrophysical environments (Lazarian 2005; Santos-Lima et al. 2010). Rapid magnetic diffusion happens in numerical codes, although the nature of numerical diffusion is different from the reconnection diffusion in astrophysical circumstances. Therefore, while numerical simulations may probably reproduce features of the astrophysical reality, the degree of their correspondence is an issue of further studies. An encouraging fact, however, is that as “reconnection diffusion” depends on the large-scale turbulent eddies, the reproduction of the entire cascade in the numerical simulations is not necessary. This work also justifies why one can study clumps with one fluid code, i.e., without including ambipolar diffusion effects.

We show that the degree of elongation of clumps can vary substantially. Identification of clumps and their evolution, including changes of the clump shapes, requires further studies.

Our present study does not include self-gravity and therefore cannot formally be applied to the self-gravitating GMCs. However, one can gain insight into the behavior of GMCs and why they can survive longer than the crossing time. Indeed, our results suggest that the accumulation of matter in GMCs happens on the timescale of the large-scale turbulent flow, L/v_L , where L is an injection scale of the turbulent motions and v_L is the velocity at the injection scale. Taking $L \approx 100$ pc and $v_L \approx 10$ km s $^{-1}$, one gets the timescale $\sim 10^7$ yr, which is a very crude estimate taking into account the approximate nature of the estimates,⁴ though it is in agreement with the observational estimative of Blitz & Shu (1980). On this timescale the GMCs are likely to be dispersed through the feedback from SF and star evolution, which resembles a pre-turbulence paradigm of GMC evolution. In addition, there is no problem explaining the existence of turbulence in GMCs, as in this picture they are being formed throughout their entire existence rather than being static entities that are relaxing their internal motions. While the turbulent formation of GMCs is not a new concept (see Ballesteros-Paredes et al. 1999), we believe that our study of clump evolution provides it more solid ground and justification.

5. SUMMARY

In this paper, we obtained the following results:

1. The magnetization of clumps, compared to the thermal pressure, increases with the mass of the clumps.
2. The lifetime of a clump scale is not limited by the sound crossing time on the scale of the clump, but is determined by the existence of the large-scale converging flow with clumps surviving many Alfvén and sonic crossing times.
3. Our model of clumps predicts that the lifetime of clumps scales linearly with the column density, which corresponds well to our numerical simulations.

The authors thank the anonymous referee for helping to improve this paper. A.L. and D.F.-G. thank the financial support of the Center for Magnetic Self-Organization in Astrophysical and Laboratory Plasmas, NSF grant AST 0808118, and the Brazilian agency FAPESP (No. 2009/10102-0).

⁴ Observational studies of turbulence using velocity channel analysis and velocity coordinate spectrum techniques (see Lazarian 2009 and references therein) should provide more precise estimates of the turbulent velocities.

REFERENCES

- Armstrong, J. W., Rickett, B. J., & Spangler, S. R. 1995, *ApJ*, **443**, 209
- Ballesteros-Paredes, J., Vázquez-Semadeni, E., & Scalo, J. 1999, *ApJ*, **515**, 286
- Beresnyak, A., Lazarian, A., & Cho, J. 2005, *ApJ*, **624**, 93
- Blitz, L., & Shu, F. 1980, *ApJ*, **238**, 148
- Blitz, L., & Williams, J. P. 1997, *ApJ*, **488**, L145
- Bonazzola, S., Heyvaerts, J., Falgarone, E., Perault, M., & Puget, J. L. 1987, *A&A*, **172**, 293
- Burkhart, B., Falceta-Gonçalves, D., Kowal, G., & Lazarian, A. 2009, *ApJ*, **693**, 250
- Chepurnov, A., & Lazarian, A. 2010, *ApJ*, **710**, 853
- Cho, J., & Lazarian, A. 2002, *Phys. Rev. Lett.*, **88**, 245001
- Cho, J., & Lazarian, A. 2003, *MNRAS*, **345**, 325
- Churchwell, E. 2002, *ARA&A*, **40**, 27
- Cowie, L. L., & McKee, C. F. 1977, *ApJ*, **211**, 135
- Elmegreen, B. G. 1993, *ApJ*, **419**, L29
- Elmegreen, B. G., & Mathieu, R. D. 1983, *MNRAS*, **203**, 305
- Elmegreen, B. G., & Scalo, J. 2004, *ARA&A*, **42**, 211
- Falceta-Gonçalves, D., Caproni, A., Abraham, Z., Teixeira, D. M., & de Gouveia Dal Pino, E. M. 2010a, *ApJ*, **713**, L74
- Falceta-Gonçalves, D., de Gouveia Dal Pino, E. M., Gallagher, J. S., & Lazarian, A. 2010b, *ApJ*, **708**, L57
- Falceta-Gonçalves, D., de Juli, M., & Jatenco-Pereira, V. 2003, *ApJ*, **597**, 970
- Falceta-Gonçalves, D., Lazarian, A., & Kowal, G. 2008, *ApJ*, **679**, 537
- Falceta-Gonçalves, D., Lazarian, A., & Houde, M. 2010c, *ApJ*, **713**, 1376
- Galván-Madrid, R., Vázquez-Semadeni, E., Kim, J., & Ballesteros-Paredes, J. 2007, *ApJ*, **670**, 480
- Gammie, C., & Ostriker, E. 1996, *ApJ*, **466**, 814
- Goldreich, P., & Sridhar, S. 1995, *ApJ*, **438**, 763
- Kamaya, H. 1996, *ApJ*, **466**, L99
- Kirk, J. M., Ward-Thompson, D., & Andre, P. 2005, *MNRAS*, **360**, 1506
- Kowal, G., & Lazarian, A. 2010, *ApJ*, **720**, 742
- Kowal, G., Lazarian, A., & Beresniak, A. 2007, *ApJ*, **658**, 423
- Kowal, G., Lazarian, A., Vishniac, E. T., & Otmianowska-Mazur, K. 2009, *ApJ*, **700**, 63
- Larson, R. B. 1981, *MNRAS*, **194**, 809
- Lazarian, A. 2005, in AIP Conf. Proc. 784, Magnetic Fields in the Universe: From Laboratory and Stars to Primordial Structures, ed. E. M. de Gouveia Dal Pino, G. Lugones, & A. Lazarian (Melville, NY: AIP), **42**
- Lazarian, A. 2009, *Space Sci. Rev.*, **143**, 357
- Lazarian, A., & Vishniac, E. T. 1999, *ApJ*, **517**, 700
- Lazarian, A., Vishniac, E. T., & Cho, J. 2004, *ApJ*, **603**, 180
- Leão, M. R. M., de Gouveia Dal Pino, E. M., Falceta-Gonçalves, D., Melioli, C., & Geraissate, F. G. 2009, *MNRAS*, **394**, 157
- Li, H.-B., & Houde, M. 2008, *ApJ*, **677**, 1151
- Mac Low, M.-M., & Klessen, R. S. 2004, *Rev. Mod. Phys.*, **76**, 125
- Martin, C., Heyvaerts, J., & Priest, E. 1997, *A&A*, **326**, 1176
- McKee, C., & Zweibel, E. 1995, *ApJ*, **440**, 686
- Mestel, L., & Spitzer, L. 1956, *MNRAS*, **116**, 503
- Padoan, P., Goodman, A. A., & Juvela, M. 2003, *ApJ*, **588**, 881
- Padoan, P., & Nordlund, A. 1999, *ApJ*, **526**, 279
- Pittard, J. M., Hartquist, T. W., & Falle, S. A. E. G. 2010, *MNRAS*, **405**, 821
- Santos-Lima, R., Lazarian, A., de Gouveia Dal Pino, E. M., & Cho, J. 2010, *ApJ*, **714**, 442
- Schmidt, W., Kern, S. A. W., Federrath, C., & Klessen, R. S. 2010, *A&A*, **516**, 25
- Shu, F. H., Adams, F. C., & Lizano, S. 1987, *ARA&A*, **25**, 23
- Vázquez-Semadeni, E., Ballesteros-Paredes, J., & Rodríguez, L. F. 1997, *ApJ*, **474**, 292
- Vázquez-Semadeni, E., Kim, J., Shadmehri, M., & Ballesteros-Paredes, J. 2005, *ApJ*, **618**, 344
- Xie, T., Mundy, L. G., Vogel, S. N., & Hofner, P. 1996, *ApJ*, **473**, L131